Solid-State Electronics Pergamon Press 1968. Vol. 11, pp. 117–128. Printed in Great Britain

ZENER AND AVALANCHE BREAKDOWN IN SILICON ALLOYED *p–n* JUNCTIONS—II

EFFECT OF TEMPERATURE ON THE REVERSE CHARACTERISTICS AND CRITERIA FOR DISTINGUISHING BETWEEN THE TWO BREAKDOWN MECHANISMS

M. SINGH TYAGI

Institut für Halbleitertechnik der Technischen Hochschule, Aachen, Germany

(*Received* 29 *May* 1967)

Abstract—The effect of temperature on the reverse current and breakdown voltage of silicon *p–n* junctions for a wide range of breakdown voltages has been investigated and the criteria for differentiating the Zener breakdown from avalanche breakdown have been presented. Narrow *p–n* junctions with soft characteristics have a temperature insensitive reverse current, contributed by internal field emission and show a negative temperature coefficient β of breakdown voltage which is determined up to large extent by the available phonon density present in tunnelling transitions. Wider junctions with $V_B > 13$ V show a highly temperature sensitive current and a positive value of β, which is in good agreement with the avalanche multiplication theory. For values of V_B from 3·5 to 13 V there is a transition region from Zener to avalanche type of breakdown in which the temperature dependence of the reverse characteristics is complex and cannot be accounted by a single mechanism. Apart from the temperature dependence of breakdown voltage such properties as generation of microplasma noise, dependence of breakdown voltage on impurity concentration, space-charge layer width and maximum field strength at breakdown have been found to show distinct differences between Zener and avalanche regions and give a further support to the conclusions reached from the temperature studies.

Résumé—L'effet de température sur le courant inverse et la tension de rupture des jonctions *p–n* en silicium pour une gamme étendue de tensions de rupture a été examiné et les critères pour différencier la rupture Zener de la rupture à avalanche ont été présentés. Les jonctions *p–n* étroites ayant des caractéristiques molles ont un courant inverse insensible à la température contribué par les émissions de champ interne et démontrent un coefficient de température négatif pour la tension de rupture qui est déterminée largement par la densité de phonons disponibles qui est présente dans les transitions à tunnel. Des jonctions plus larges ayant $V_B > 13$ V démontrent un courant très sensible à la temperature et une valeur positive de β qui est en bon accord avec la théorie de multiplication à avalanche. Pour les valeurs de V_B de 3,5 à 13 V il y a une région de transition du type de rupture Zener au type à avalanche dans laquelle la dépendance de température des caractéristiques inverses est compliquée et ne peut être expliquée par un simple mécanisme. A part la dépendance de la tension de rupture sur la température, des propriétés telles que la génération du bruit microplasma, la dépendance de la tension de rupture sur la concentration d'impuretés, la largeur de la couche de la charge d'espace et la force de champ à la rupture ont été trouvées comme démontrant des différences distinctes entre les régions Zener et à avalanche et appuient les conclusions tirées des études de température.

Zusammenfassung—Der Einfluss der Temperatur auf den Sperrstrom und die Durchbruchspannung bei legiertem Silizium *pn*-Übergängen in einem weiten Durchbruchspannungsbereich wird untersucht und die Kriterien zur Unterscheidung zwischen Zener- und Lawinendurchbruch werden behandelt. *Pn*-Übergänge mit kleinen Sperrschichtweiten zeigen weiche Kennlinien und einen temperaturunempfindlichen Sperrstrom, der durch innere Feldemission ausgelöst wird.

Dabei ergibt sich ein negativer Temperaturkoeffizient β der Durchbruchspannung, der hauptsächlich durch die verfügbare Phononendichte bei indirektem Tunneln bestimmt wird. Breite Sperrschichten mit Durchbruchspannung $V_B > 13$ V sind durch eine starke Temperaturabhängigkeit des Sperrstromes und durch einen negativen Wert von β bei guter Übereinstimmung mit der Lawinenmultiplikationstheorie gekennzeichnet. Für Werte von V_B zwischen 3, 5 und 13 V findet ein Übergang vom Zener- zum Lawinendurchbruch statt, in dem das Temperaturverhalten der Kennlinie komplizierter ist und nicht auf einen einzelnen Mechanismus zurückgeführt werden kann. Zwischen dem Zener- und Lawinendurchbruch beobachtet man ausserdem deutliche Unterschiede von Eigenschaften wie Erzeugung von Mikroplasmen-Rauschen, Abhängigkeit der Durchbruchspannung von Störstellen-Konzentration, sowie Sperrschichtweite und maximaler Feldstärke beim Durchbruch.

1. INTRODUCTION

IN PAPER I an analysis of the reverse characteristics of p–n junctions in the light of internal field emission and avalanche multiplication phenomenon has been undertaken. This paper is concerned with the investigation of the effect of temperature on the reverse characteristics and the criteria for distinguishing between the two mechanisms of breakdown. Reference to some of the results of paper I will be made from time to time.

2. TEMPERATURE DEPENDENCE OF REVERSE CHARACTERISTICS

(*a*) *Reverse saturation region*

(*i*) *Experimental results.* Reverse currents of samples Nos. 1, 2 and 3 are so insensitive to the temperature that a change in temperature by about 200°C increases the current only by a factor of 2 or 3. Moreover at a constant value of current the reverse voltage decreases with temperature. For samples Nos. 4–7 also, the reverse currents are relatively insensitive to the temperature, but this temperature dependence increases with increasing reverse voltage. The change in voltage with temperature $(dV/dT)_I$ is negative at low currents and positive at high currents (see Fig. 7 of paper I). The softness of the characteristic also increases with temperature. This tendency is clearly visible for the sample No. 7. At low temperature the characteristic is hard and a well defined breakover point exists. At 80°C the characteristic becomes soft. Samples No. 12–17 show a rapid change in current with temperature, while the temperature dependence for samples No. 8–11 is still smaller than those of No. 12–17.

(*ii*) *Discussion.* The temperature insensitivity of the reverse current in samples No. 1–7 is attributed to the fact that the reverse current in these samples is a field emitted current whose temperature dependence is controlled mainly by the change in the tunnelling probability Z with the temperature. Because $Z \approx \exp(-\alpha E_g^{3/2}/F)$ this tunnel current will depend exponentially on the energy gap E_g. The band gap E_g decreases slowly with increasing temperature so that Z and also the tunnel current will increase slowly with temperature.

Similar considerations can also be applied to the diodes No. 8–11. As shown in paper I, these diodes show a field emitted current component along with the reverse saturation and other current components. Because the temperature dependence of the field emitted current is smaller than that of the other current components, the total current does not depend so strongly on temperature as in case of diodes where no Zener current component is present.

Theoretically the temperature dependence of the thermally generated saturation current is given by $I(T) \approx T^3 e^{-E_g/kT}$. The observed temperature dependence of the reverse current in silicon p–n junctions is smaller, because the thermal current is swamped out by less temperature dependent leakage current and the generation–recombination current I_{rg}. It has been found by measurements that for each 10°C rise in temperature the reverse current doubles itself.[1] This behaviour is shown approximately by the samples No. 12–17, which do not show a Zener current component.

(*b*) *Breakdown region*

(*i*) *Temperature coefficient of breakdown voltage.* For silicon p–n junctions it has been found by McKAY[2] that the breakdown voltage V_B at a

temperature T is given by the relation

$$V_B = V_{B0}[1+\beta(T-T_0)]. \qquad (1)$$

Here V_{B0} is the breakdown voltage at room temperature, T_0, and β is the temperature coefficient of breakdown voltage. McKay reports that when breakdown occurs by avalanche mechanism the value of β is $8{\cdot}8\times10^{-4}\,°C^{-1}$ and remains constant between a temperature range of 25 to $-196°C$. This means that the breakdown voltage varies linearly with temperature.

(*ii*) *Experimental results.* The measured temperature dependence of breakdown voltage for different samples is quite different depending on the breakdown mechanism.

For samples which show a pure Zener type of breakdown β is negative and increases with increasing breakdown voltage. Figure 1 shows the temperature dependence of reverse voltage in the neighbourhood of breakdown for two samples with breakdown voltage < 1 V. The voltage

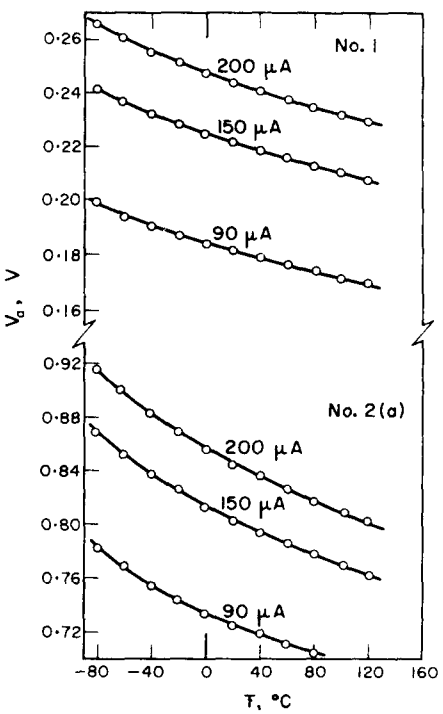

FIG. 1. Variation of breakdown voltage with ambient temperature for different values of current (samples with Zener breakdown).

measurements were made with a potentiometer with a probable error of $\pm0{\cdot}1$ mV. It is seen from Fig. 1 that the breakdown voltage decreases non-linearly with temperature, showing that the value of β for these samples is not constant but is a function of temperature. A similar behaviour has also been found by CHYNOWETH *et al.*[3]

Samples No. 7–17 show a positive value of β, which increases with breakdown voltage, first rapidly, and then slowly (see Fig. 5). These samples include the diodes with pure avalanche breakdown and also those of the transition region. Figure 2 shows the breakdown voltage of samples

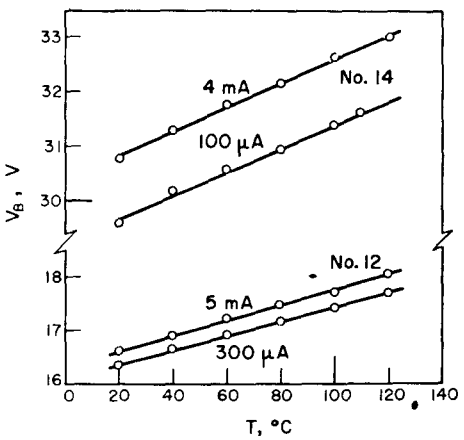

FIG. 2. Variation of breakdown voltage with ambient temperature for samples with avalanche breakdown.

No. 12 and 14 plotted as a function of temperature. The measurements were made by pulse method with a probable error of ±5 mV. It is seen from Fig. 2 that the breakdown voltage increases linearly with temperature.

(*iii*) *Zener breakdown.* For samples with Zener breakdown the reverse characteristic is soft and the breakdown voltage is defined as the voltage corresponding to a specified value of the reverse current. Equation (7) of paper I shows that the constant current condition is given by

$$\left(N\frac{Z_A}{Z_E}+1\right)Z_E = \text{const.} \qquad (2)$$

At room temperature and above, the phonon density N is large so that the constant current condition becomes

$$NZ_A = \text{const.} \qquad (3)$$

After substituting the value of Z for an abrupt junction we have

$$N \exp[-W_1 \alpha E_g^{3/2}/2(V_a+\phi)^{1/2}] = \text{const.} \tag{4}$$

If W_1 and α are treated as temperature independent quantities, equation (4) shows that the temperature dependence of V_a will be determined by the temperature dependence of E_g and that of the phonon density N. To see if the temperature dependence of V_a could be accounted by the temperature variation of E_g alone, we disregard the effect of phonon cooperation and treat N as constant. We thus have

$$\frac{W_1 \alpha E_g^{3/2}}{2(V_a+\phi)^{1/2}} = \text{const.} \tag{5}$$

or

$$\frac{E_g^{3/2}}{(V_a+V_g)^{1/2}} = \text{const.} \tag{6}$$

Here ϕ has been put equal to V_g, the voltage corresponding to the band gap E_g.

The voltage V_a for constant current values has been measured for diodes No. 1 and No. 2(a) in temperature range from -80°C to 120°C at every 20°C interval (see Fig. 1). The values of E_g at these temperatures have been calculated by using the results of MACFARLANE *et al.*[4] When these values of E_g and V_a are substituted in equation (6) it is found that the quantity

$$\frac{E_g^{3/2}}{(V_g+V_a)^{1/2}}$$

does not remain constant but increases with temperature which shows that the temperature variation of V_a is not contained in E_g alone, but is also influenced by the phonon density N. The temperature dependence of N is given by

$$N = \frac{N_0}{\left(\exp\frac{\hbar\omega}{kT} - 1\right)}. \tag{7}$$

Substituting this value in equation (4) one obtains

$$\ln\left(\exp\frac{\hbar\omega}{kT} - 1\right) + \frac{W_1 \alpha q^{3/2} V_g^{3/2}}{2(V_g+V_a)^{1/2}} = \text{const.} \tag{8}$$

Noting that for the diodes under consideration $\phi \approx V_g = E_g/q$ and for sample No. 1 $V_a \ll \phi$ we obtain

$$\ln\left(\exp\frac{\hbar\omega}{kT} - 1\right) + \frac{W_1 \alpha q^{3/2}}{4}(2V_g - V_a) = \text{const.} \tag{9}$$

For the lowest acoustical phonon energy (for silicon = 0·019 eV) the function

$$\log_{10}\left(\exp\frac{\hbar\omega}{kT} - 1\right)$$

has been plotted against $(2V_g - V_a)$ in Fig. 3 for three different current values. The temperature dependence of E_g was calculated up to 10^{-4} eV by using the results of MACFARLANE *et al.*[4]

In the temperature range between 293 and 393°K the plots are linear as is to be expected. At lower temperatures this linear relation does not hold because the phonon density N is small and the assumption $N(Z_A/Z_E) \gg 1$ is no longer valid. The slope of the lines is about 4 V^{-1}. This gives a value of $\alpha E_g^{3/2} = 3{\cdot}3 \times 10^7$ V/cm. This value is in good agreement with those reported in Table 2 of paper I.

For diode No. 2(a), the relation $V_g \gg V_a$ is not valid so that equation (8) is to be used. A plot of

$$\log_{10}\left(\exp\frac{\hbar\omega}{kT} - 1\right)$$

against $E_g^{3/2}/(V_g+V_a)^{1/2}$ for this diode is shown in Fig. 4, which is again linear in the temperature range between 293 and 393°K. The value of $\alpha E_g^{3/2}$ calculated from the slope of this line is $2{\cdot}6 \times 10^7$ V/cm.

In the above analysis it has been assumed that only the acoustical phonons are contributing to the current. This assumption, however, is not justified by the experiments. If instead of the acoustical phonon energy the transverse optical phonon energy $\hbar\omega/kT = 0{\cdot}063$ eV[5] is substituted in equations (8) and (9) the plots of Figs. 4 and 3 can again be approximated by straight lines for temperatures between 293 and 393°K. The values of $\alpha E_g^{3/2}$ from these new plots are $6{\cdot}1 \times 10^7$ V/cm for diode No. 1 and $4{\cdot}4 \times 10^7$ V/cm for diode No. 2(a). These values

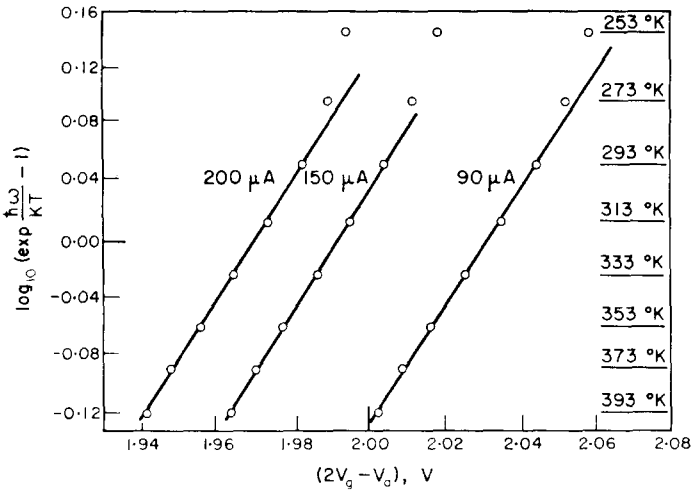

FIG. 3. Temperature dependence of $(2V_g - V_a)$ for sample No. 1 with current as parameter.

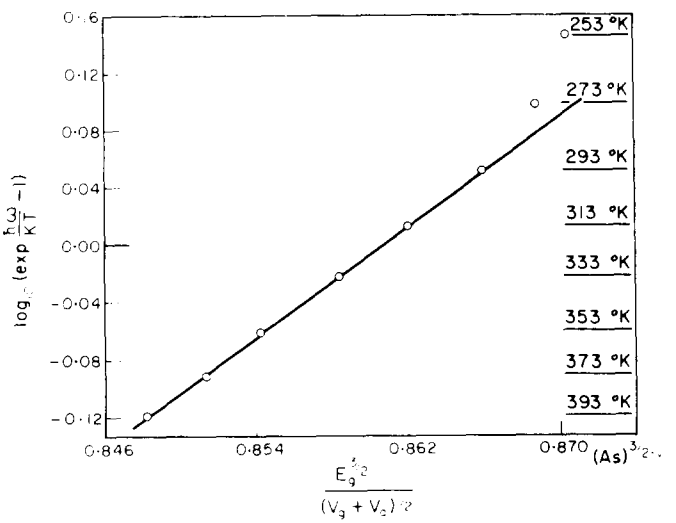

FIG. 4. Temperature dependence of $E_g^{3/2}/(V_g + V_a)^{1/2}$ for sample No. 2(a).

are considerably higher than those found previously. Moreover in the above calculations ϕ has been replaced by V_g so that the calculated values of $\alpha E_g^{3/2}$ should be about 4×10^7 V/cm, slightly less than those found from the analysis of the reverse characteristics for calculated values of ϕ (see Table 2, paper I). It thus seems that both the acoustical as well as optical phonons contribute to the current.

The above discussion shows that for those silicon p–n junctions in which breakdown occurs due to Zener effect a unique value of the temperature coefficient β of breakdown voltage can not be derived. This quantity is a function of the temperature and also of the breakdown voltage. However a rough estimate of β is possible. If the effect of phonon cooperation is neglected and only the change in the breakdown voltage due

to the change in the band gap with the temperature is considered, equation (6) gives

$$E_g^3 = \text{const.}(V_B+\phi). \tag{10}$$

where V_a has been replaced by the breakdown voltage V_B. After differentiating this equation with respect to temperature we obtain

$$\frac{3}{E_g}\frac{\partial E_g}{\partial T} = \frac{1}{(V_B+\phi)}\cdot\left(\frac{\partial V_B}{\partial T}\right). \tag{11}$$

In the derivation of equation (11) ϕ has been treated as independent of temperature. In the temperature range between 20 and 120°C the measurements of MACFARLANE *et al.*[4] show that the quantity

$$\frac{1}{E_{g0}}\frac{\partial E_g}{\partial T} = -2{\cdot}5\times10^{-4}\,^{\circ}\mathrm{C}^{-1}.$$

This gives

$$\beta = \frac{1}{(V_{B0}+\phi)}\left(\frac{\partial V_B}{\partial T}\right) = -7{\cdot}5\times10^{-4}\,^{\circ}\mathrm{C}^{-1}.$$

The quantities E_{g0} and V_{B0} are the values of E_g and V_B at room temperature. The measured values of β will be larger than this because of the relation (4). The lower values of β for samples No. 2 and 3 in Table 1 are due to the fact, that here ϕ has been neglected and β is defined as

$$\beta = \frac{1}{V_{B0}}\left(\frac{\partial V_B}{\partial T}\right).$$

If $(\partial V_B/\partial T)$ is divided by $(V_{B0}+\phi)$ the obtained values are $-4{\cdot}3\times10^{-4}\,^{\circ}\mathrm{C}^{-1}$ and $-5{\cdot}5\times10^{-4}\,^{\circ}\mathrm{C}^{-1}$ respectively. For lower temperatures where the assumption $N(Z_A/Z_E)\gg 1$ does not hold, β is usually smaller than the above value.

(*iv*) *Avalanche breakdown.* In case of avalanche breakdown the voltage at which the multiplication factor M becomes infinite is the breakdown voltage. The factors that determine the voltage that must be applied to obtain a given value of M are the built in voltage ϕ, the threshold energy E_i that a carrier is required to have in order to produce an electron–hole pair and the energy E_R, that a carrier loses to the lattice during its travel through the space charge layer.

The temperature dependence of the voltage at which a specified M value is reached—and hence also of the breakdown voltage—will be determined by all these factors. Considering these factors individually, it is found that E_i does not depend on temperature and ϕ decreases slightly with the temperature so that the only important factor that influences the multiplication is the energy loss E_R. With increasing temperature this energy loss will increase, reducing in turn the ionization rate. To compensate this loss the field strength and that means the applied voltage must be increased to get a specific value of M.

A rough estimate of the temperature coefficient of ionization rates can be obtained with the help of equation (34) of paper I. After substituting $M=\infty$ we obtain

$$1 = \frac{2(V_B+\phi)}{b}\alpha_x \exp[-bW_1/2(V_B+\phi)^{1/2}]. \tag{12}$$

If ϕ and W_1 are treated as temperature independent quantities, α_x and b must vary with temperature to explain the observed temperature dependence of V.

Disregarding the nature of α_x and b we treat them as two independent parameters and see how they affect the breakdown voltage individually. If α_x is kept constant it is found that in going from 20 to 120 C, b must be increased by about 5–6 per cent above its room temperature value of $1{\cdot}65\times10^6$ V/cm in order to account for the increase in the breakdown voltage. If on the other hand b is kept constant a reduction of 15–21 per cent of its room temperature value of 9×10^5 cm^{-1} is required for α_x. Both these changes give an average temperature coefficient of ionization rate equal to $-18\times10^{-4}\,^{\circ}\mathrm{C}^{-1}$. This figure compares satisfactorily with $-20\times10^{-4}\,^{\circ}\mathrm{C}^{-1}$, reported by MCKAY.[2] To get some insight into the problem and to compare the measured results with the theory it is better to consider equation (31) of paper I. For $M=\infty$ this equation can be written as

$$\gamma = \exp[(\gamma-1)W_{\text{eff}}(\alpha_x)_b \exp(-b/F_B)]. \tag{13}$$

On the assumption that γ and W_{eff} are not significantly influenced by temperature we must

have

$$(\alpha_\infty)_p \exp(-b/F_B) = \text{const.} \qquad (14)$$

where F_B is the maximum field strength in the junction at breakdown.

If one is confined to moderate field strengths and uses the values

$$\alpha_\infty = \frac{qF}{rE_r} \quad \text{and} \quad b = \frac{E_i}{ql_r}$$

as suggested by SHOCKLEY[5] condition (14) becomes

$$\frac{qF_B}{rE_r} \exp(-b/F_B) = \text{const.} \qquad (15)$$

Here q is the electron charge, l_r is the mean free path for phonon scattering and rE_r is a constant independent of temperature. Differentiating equation (15) with respect to temperature the following relation is obtained

$$\frac{1}{b}\left(\frac{\partial b}{\partial T}\right) = \frac{1}{F_B}\frac{\partial F_B}{\partial T}\left[1+\frac{F_B}{b}\right]. \qquad (16)$$

Substituting the value of b on the left-hand side of (16) gives

$$\frac{1}{F_B} = \frac{-\frac{1}{l_r}\left(\frac{\partial l_r}{\partial T}\right)}{\left(1+\frac{F_B}{b}\right)}. \qquad (17)$$

LEE *et al.*[6] have estimated the value of l_r at 100 and 300°K. If a linear variation in l_r between these temperatures is assumed we get

$$\frac{1}{l_{r0}}\left(\frac{\partial l_r}{\partial T}\right) = -5{\cdot}15 \times 10^{-3}\,{}^\circ\text{C}^{-1}. \qquad (18)$$

For an abrupt p–n junction we have

$$\beta = \frac{1}{V_{B0}}\left(\frac{\partial V_B}{\partial T}\right) = \frac{2}{F_{B0}}\left(\frac{\partial F_B}{\partial T}\right). \qquad (19)$$

This gives

$$\beta = \frac{1{\cdot}03 \times 10^{-3}}{\left(1+\frac{F_B}{b}\right)}. \qquad (20)$$

The index 0 signifies the quantities at room temperature. Equation (20) predicts that the temperature coefficient of breakdown voltage increases slowly as F_B decreases. This is the general behaviour shown by p–n junctions. In practice β will be influenced by the junction geometry, dislocations and by the thermal resistance of the diode so that small deviations from the above predicted ideal behaviour are possible. The voltage dependence of β is plotted in Fig. 5. In spite of all the approximations in the above analysis a good agreement between the measured and calculated values is found.

With increasing temperature, therefore, the mean free path of phonon scattering decreases

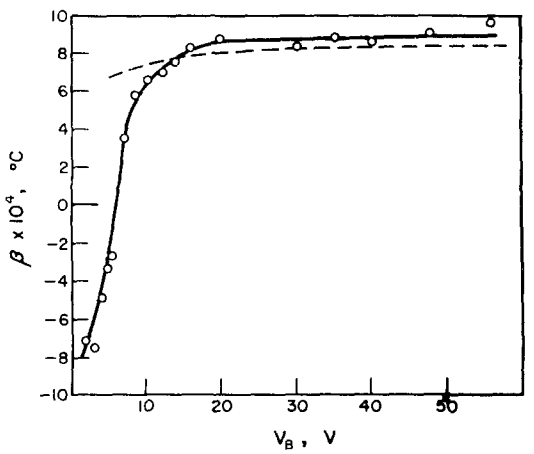

FIG. 5. Temperature coefficient of breakdown voltage as function of breakdown voltage at 20°C. ○ Measured points; – – – – Calculated on the basis of the theory of avalanche breakdown.

so that during its transit through the space-charge region a carrier will have more collisions, thus losing more energy to the lattice. This will increase the breakdown voltage as explained above.

(*v*) *Transition region between Zener and avalanche breakdown.* In the transition region between Zener and avalanche breakdown the temperature coefficient of breakdown voltage is determined by the relative intensity of the two effects at breakdown. The value of β is greater than that for Zener breakdown and smaller than that for pure avalanche breakdown. In the transition region the field-emitted carriers also obtain avalanche multiplication and hence the two effects present complex

thermal characteristics. Hence from a theoretical consideration no simple figure of temperature coefficient should result for a junction whose breakdown voltage lies in the transition region.

From the above consideration it is possible to understand why the characteristics of junctions such as No. 6, 7 and 8 (see Fig. 7 of paper I) become softer at higher temperatures. At low temperatures both the band gap and the phonon mean free path are larger than that at higher temperature. The tunnelling probability is therefore smaller and the avalanche multiplication is larger so that the reverse current will have a larger component of avalanche multiplication current and the breakdown will be mainly due to avalanche mechanism, giving a harder characteristic. With increasing temperature E_g and l_r will be reduced so that the carrier multiplication factor M will decrease but due to the increase in the tunnelling probability the field emitted current component will increase and the breakdown will be caused by internal field emission. This will make the characteristic soft.

3. CRITERIA FOR DISTINGUISHING BETWEEN THE TWO BREAKDOWN MECHANISMS

Table 1 shows some of the important data determined for the measured samples. Some of these data are helpful in distinguishing between the two breakdown mechanisms.

(a) *Temperature coefficient of breakdown voltage*

As has been discussed above the temperature coefficient of breakdown voltage is positive for junctions with avalanche breakdown and its value is usually larger than $7\times10^{-4}\,^{\circ}C^{-1}$. For samples with Zener breakdown β is negative. The measurement of the temperature dependence of breakdown voltage gives a very reliable information about the type of breakdown.

Figure 5 shows the measured values of β as a function of breakdown voltage at 20°C in the temperature range 20–120°C. For comparison the values of β calculated with the help of equation (20), after substituting $b = 1{\cdot}65\times10^{6}$ V/cm, have also been shown (dotted curve). For low values of V_B, β is negative and increases with increasing breakdown voltage, reaching zero at about 6 V. For $V_B > 6$ V β is positive and reaches almost its saturation value at about 16 V. The calculated curve gives only positive values of β and cuts the measured curve at a voltage of about 13 V. From 16 V on the two curves run almost parallel indicating that the breakdown in junctions with $V_B \geq 16$ V can be explained by the avalanche mechanism. For $V_B < 13$ V the measured values

Table 1. Some useful data of the measured samples

Sample No.	$(V_B+\phi)$, V	Junction area $\times10^4$, cm^2	$W_1\times10^8$, cm-V$^{-1/2}$		$W_B\times10^8$, cm	$F_B\times10^{-5}$, V/cm	$\times10^4$, °C^{-1}
			Calc.	Meas.			
1	1·14	1·05	117	129	152	18·7	—
2	2·36	1·20	171	197	326	15·5	−7·1
3	4·63	29·3	—	271	620	15·1	−7·3
4	5·15	16·6	—	307	736	14·6	−4·7
5	5·25	28·2	—	317	741	14·2	−3·4
6	6·25	31·1	—	344	905	14·0	−2·8
7	7·60	20·6	415	441	1140	13·3	3·6
8	8·75	37·4	—	514	1365	11·6	5·8
9	10·91	10·7	725	721	2375	9·23	6·6
10	12·52	5·05	910	1009	3530	7·10	7·0
11	14·63	6·9	1280	1275	4617	6·35	7·5
12	16·99	6·5	1480	1600	6620	5·11	8·5
13	20·36	36·6	1850	1910	8920	4·60	8·8
14	30·18	10·8	2570	2610	14400	4·17	8·3
15	41·02	29·3	3300	3430	22300	3·68	8·4
16	46·73	121·0	—	4530	16300	4·20	8·9
17	55·81	11·8	3710	4680	37000	2·98	9·7

of β are lower than the calculated values. This shows that the breakdown in these diodes cannot be explained by the avalanche mechanism alone, but is caused by a combination of both—the internal field emission and avalanche effect. These observations are in agreement with those reported in paper I.

(b) Breakdown instability

Instability and pulsing mechanism at the onset of breakdown associated with considerable noise and a small region of apparent negative resistance are the necessary accompaniment of avalanche breakdown. No negative resistance region is observed in Zener type of breakdown. These pulses are observed only in diodes with $V_B \gtrsim 8$ V. One can conclude, therefore that at 8 V the avalanche mechanism will dominate over internal field emission.[2,7]

(c) Specific resistivity of the base crystal

A relation between W_1 and the donor density N_d and the acceptor density N_a on n and p sides of the junction is given by

$$W_1^2 = \frac{2\epsilon}{q}\left[\frac{1}{N_d}+\frac{1}{N_a}\right] = \frac{2\epsilon}{qN_I}.$$

After substituting $q = 1{\cdot}6\times10^{-19}$ C and $\epsilon = 1{\cdot}11\times10^{-12}$ F/cm one obtains

$$W_1 = \left(\frac{1{\cdot}38\times10^{7}}{N_I}\right)^{1/2} \qquad (21)$$

Here W_1 is expressed in cm $V^{-1/2}$ and N_I in cm^{-3}.

For those samples whose base resistivity was known, the values of N_d were determined from the curves given by IRVIN[8], and W_1 was calculated with the help of the above equation by taking $N_a = 2{\cdot}3\times10^{19}$.[9] The calculated and measured values of W_1 are shown in Table 1. In spite of some uncertainty in the exact value of the resistivity of the individual diode elements, the agreement between the calculated and the measured values of W_1 is good. For all the samples, except No. 1 $N_a \gg N_d$, so that W_1 is a measure of the doping and in turn also of the resistivity of the base crystal.

For an abrupt p–n junction we have

$$(V_B+\phi) = \frac{F_B^2 W_1}{4}. \qquad (22)$$

For $F_B = 1{\cdot}4\times10^6$ V/cm, a value obtained from Shockley's equation for Zener breakdown in silicon,[10,11] equation (22) is plotted in Fig. 6.

A relation between W_1 and breakdown voltage in case of avalanche breakdown can be obtained

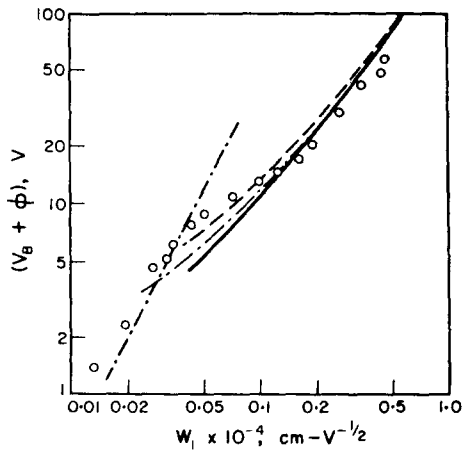

FIG. 6. Breakdown voltage as a function of width constant W_1. ○ Measured points; —·— Calculated for Zener breakdown; ——— Calculated for avalanche breakdown according to equation (23), – – – Calculated for avalanche breakdown according to equation (24); —·— data of MILLER[13].

from equation (13) or (12). After substituting $\alpha_\infty = 9\times10^5\ cm^{-1}$ and $b = 1{\cdot}65\times10^6$ V/cm in equation (13) we obtain

$$W_1 = 2{\cdot}8\times10^{-6}(V_B+\phi)^{1/2}[\log_{10}(V_B+\phi)+0{\cdot}04]. \qquad (23)$$

If one substitutes the values

$$(\alpha_\infty)_p = 5{\cdot}5\times10^5\ cm^{-1},$$

$b = 1{\cdot}65\times10^6$ V/cm and $\gamma = 3{\cdot}3$[12] in equation (12) one gets

$$9{\cdot}5\times10^{-7}\exp\frac{8{\cdot}25\times10^5}{(V_B+\phi)^{1/2}} = \left(\frac{W_{\text{eff}}}{W}\right)W_1(V_a+\phi)^{1/2}. \qquad (24)$$

In these equations W_1 is expressed in cm $V^{-1/2}$ and $(V_B+\phi)$ in volts.

Relation (23) and (24) have also been plotted in Fig. 6. The measured values of W_1 and the corresponding breakdown voltage are also shown as well as MILLER's[13] data.

It is evident that the difference between the curves obtained from equations (23) and (24) is insignificant and that the values obtained from equation (23) are in better agreement with the experimentally determined values. Due to its simplicity only equation (23) will be used in the further work. It is seen from Fig. 6 that up to a breakdown voltage of 5 V i.e. $(V_B+\phi) \approx 6$ V, the measured points lie on or above the field emission plot. For V_B in excess of 13 V i.e. $(V_B+\phi) \geq 14$ V, the measured points lie on or below the plots for avalanche breakdown. Between these two limits all the measured points lie between the two plots. This again indicates that between 5 and 13 V the two mechanisms occur simultaneously. The discrepancy between the calculated and the measured values of V_B for junctions with $V_B > 20$ V may be attributed to microplasma effects.

(*d*) *Space-charge layer width at breakdown*

The above relations can also be expressed in terms of space charge layer width W_B instead of W_1. For Zener breakdown after substituting $F_B = 1{\cdot}4 \times 10^6$ V/cm, one obtains

$$W_B = 1{\cdot}43 \times 10^{-6}(V_B+\phi). \qquad (25)$$

For avalanche breakdown we obtain

$$W_B = 2{\cdot}8 \times 10^{-6}(V_B+\phi)[\log_{10}(V_B+\phi)+0{\cdot}04]. \qquad (26)$$

Here W_B is expressed in cm and $(V_B+\phi)$ in volts.

Relations (25) and (26) are plotted in Fig. 7,

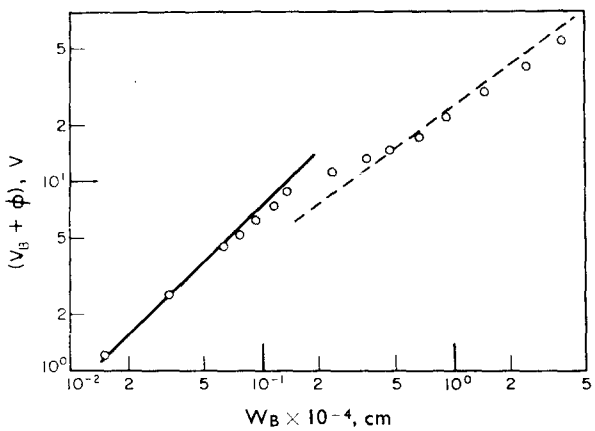

FIG. 7. Breakdown voltage as a function of the space-charge layer width at breakdown. ○ Measured points; ——— Calculated for Zener breakdown; - - - - Calculated for avalanche breakdown.

where the experimentally determined relation between W_B and $(V_B+\phi)$ has also been shown. A logarithmic plot of equation (25) is a straight line. The measured points lie on a straight line only up to a voltage $(V_B+\phi) \approx 7$ V. The slope of the straight line deviates from the calculated value, because the field strength F_B is not constant but varies with the breakdown voltage. For $V_B > 14$ V the measured points fall below the plot for avalanche breakdown.

(*e*) *Maximum field strength F_B at breakdown*

Maximum field strength at breakdown was determined for a number of samples and is plotted in Fig. 8 as a function of breakdown voltage. For an abrupt *p–n* junction the maximum field strength for avalanche breakdown can be calculated from

equation (23) and is given by

$$F_B = \frac{7{\cdot}1 \times 10^5}{\log_{10}(V_B+\phi)+0{\cdot}04}. \qquad (27)$$

This relation is also plotted in Fig. 8 (dotted curve). For voltages less than 12 V the calculated values of F_B are much lower than the measured

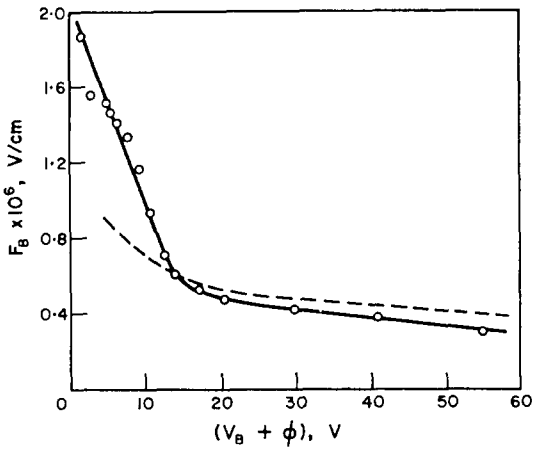

FIG. 8. Relation between maximum field strength at breakdown and breakdown voltage. ○ Measured points; - - - - Calculated for avalanche breakdown, according to equation (27).

ones. At about 14 V the calculated curve cuts the measured curve and after that the measured values are somewhat lower than the calculated

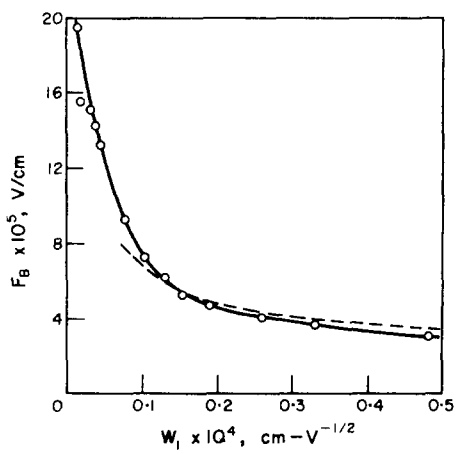

FIG. 9. Dependence of maximum field strength at breakdown on width constant W_1. ○ Measured points; - - - - Calculated for avalanche breakdown.

values. The voltage $(V_B+\phi) \approx 14$ V or $V_B = 13$ V can be taken as the upper limit for Zener breakdown.

Finally Fig. 9 shows the measured and calculated relations between W_1 and F_B. Similar conclusions can be drawn from this figure also.

4. CONCLUSIONS

The effect of temperature on the reverse characteristic and the breakdown voltage of *p–n* junctions is different for different samples depending upon the mechanism by which the current is generated and the breakdown occurs. For those junctions in which breakdown is caused by internal field emission, the reverse current is insensitive to temperature and the temperature coefficient of breakdown voltage is negative. A quantitative evaluation of the Zener voltage shows that the tunnelling transitions in silicon *p–n* junctions are indirect. In samples with avalanche breakdown the reverse current is very sensitive to the temperature and the temperature coefficient of breakdown voltage is greater than 7×10^{-4} °C^{-1}.

The values of the temperature coefficient β of breakdown voltage calculated with the help of the temperature dependence of the ionization rates show a good agreement with the measured values for diodes with $V_B > 13$ V. At lower breakdown voltages the measured values are smaller, because both the Zener and the avalanche mechanisms operate simultaneously in this voltage range. In the transition region the temperature dependence of reverse current is complex and a composite temperature coefficient of breakdown voltage results depending upon the breakdown current and the ambient temperature.

With the help of the measured ionization rates and with the knowledge of the width constants of junctions such quantities as the breakdown voltage, space-charge layer width and maximum field at breakdown can be calculated for avalanche breakdown. These quantities can also be calculated for Zener breakdown if a reasonable value of breakdown field strength is taken. Significant field emission occurs only in junctions with field strengths of 10^6 V/cm or larger and junction widths of less than 1000 Å.

A comparison of the calculated and the measured values of breakdown voltage, field strength and

junction width at breakdown shows that the breakdown in junctions with $V_B > 13$ V is due to avalanche mechanism and in junctions with $V_B < 3$ V is due to internal field emission. Between these two limits the breakdown is due to a combination of both the mechanisms.

In calculating such quantities as breakdown voltage and field strength one assumes ideal conditions and treats these quantities constant all over the space-charge layer. In practical junctions, dislocations and inhomogeneities may significantly change their values from place to place, so that an exact comparison of the theory with experiments puts stringent requirements on the fabrication technology of junction devices.

Acknowledgement—The author is indebted to Prof. Dr. HEINZ BENEKING for his constant interest, guidance and encouragement.

REFERENCES

1. W. GUGGENBÜHL, M. J. O. STRUTT and W. WUNDERLIN, *Halbleiterbauelemente*, Vol. I, p. 195 Birkenhäuser, Basel (1962).
2. K. G. MCKAY, *Phys. Rev.* **94,** 877 (1954).
3. A. G. CHYNOWETH, W. L. FELDMANN, C. A. LEE, R. A. LOGAN and G. L. PEARSON, *Phys. Rev.* **118,** 425 (1960).
4. G. G. MACFARLANE, T. P. MCLEAN, J. E. QUARRINGTON and V. ROBERTS, *Phys. Rev.* **111,** 1245 (1958).
5. W. SHOCKLEY, *Solid St. Electron.* **2,** 35 (1961).
6. C. A. LEE, R. A. LOGAN, R. L. BATDORF, J. J. KLEIMACK and W. WIEGMANN, *Phys. Rev.* **134,** 761 (1964).
7. K. S. CHAMPLIN, *J. appl. Phys.* **30,** 1039 (1959).
8. J. C. IRVIN, *Bell Syst. tech. J.* **124,** 1101 (1961).
9. R. A. LOGAN and A. G. CHYNOWETH, *Phys. Rev.* **131,** 89 (1963).
10. K. B. MCAFEE, E. J. RYDER, W. SHOCKLEY and M. SPARKS, *Phys. Rev.* **83,** 650 (1951).
11. A. G. CHYNOWETH and K. G. MCKAY, *Phys. Rev.* **106,** 418 (1957).
12. J. L. MOLL and R. VAN OVERSTRAITEN, *Solid-St. Electron.* **6,** 147 (1963).
13. S. L. MILLER, *Phys. Rev.* **105,** 1246 (1957).